

# Structure of Human Pancreatic Lipase-Related Protein 2 with the Lid in an Open Conformation<sup>†,‡</sup>

Cécilia Eydoux,<sup>§</sup> Silvia Spinelli,<sup>||</sup> Tara L. Davis,<sup>⊥</sup> John R. Walker,<sup>⊥</sup> Alma Seitova,<sup>⊥</sup> Sirano Dhe-Paganon,<sup>⊥</sup> Alain De Caro,<sup>§</sup> Christian Cambillau,<sup>\*||</sup> and Frédéric Carrière<sup>\*§</sup>

*CNRS UPR9025 Laboratoire d'Enzymologie Interfaciale et de Physiologie de la Lipolyse, Marseille, France, Laboratoire d'Architecture et Fonction des Macromolécules Biologiques, CNRS UMR6098, Aix-Marseille Université, Marseille, France, and Structural Genomics Consortium, University of Toronto, Ontario, Canada*

Received March 31, 2008; Revised Manuscript Received July 15, 2008

**ABSTRACT:** Access to the active site of pancreatic lipase (PL) is controlled by a surface loop, the lid, which normally undergoes conformational changes only upon addition of lipids or amphiphiles. Structures of PL with their lids in the open and functional conformation have required cocrystallization with amphiphiles. Here we report two crystal structures of wild-type and unglycosylated human pancreatic lipase-related protein 2 (HPLRP2) with the lid in an open conformation in the absence of amphiphiles. These structures solved independently are strikingly similar, with some residues of the lid being poorly defined in the electron-density map. The open conformation of the lid is however different from that previously observed in classical liganded PL, suggesting different kinetic properties for HPLRP2. Here we show that the HPLRP2 is directly inhibited by E600, does not present interfacial activation, and acts preferentially on substrates forming monomers or small aggregates (micelles) dispersed in solution like monoglycerides, phospholipids and galactolipids, whereas classical PL displays reverse properties and a high specificity for unsoluble substrates like triglycerides and diglycerides forming oil-in-water interfaces. These biochemical properties imply that the lid of HPLRP2 is likely to spontaneously adopt in solution the open conformation observed in the crystal structure. This open conformation generates a large cavity capable of accommodating the digalactose polar head of galactolipids, similar to that previously observed in the active site of the guinea pig PLRP2, but absent from the classical PL. Most of the structural and kinetic properties of HPLRP2 were found to be different from those of rat PLRP2, the structure of which was previously obtained with the lid in a closed conformation. Our findings illustrate the essential role of the lid in determining the substrate specificity and the mechanism of action of lipases.

Lipases (EC 3.1.1.3) are model enzymes for understanding the specific features of interfacial enzymology since they are water-soluble enzymes hydrolyzing insoluble substrates (triglycerides). Structure–function studies on various lipases have shed light on the interfacial recognition sites

present in the molecular structure of these enzymes and the conformational changes occurring in the presence of lipids and amphiphiles. In many lipases, access to the active site is controlled by a so-called lid formed by a surface loop. This lid was found to undergo a conformational change in the presence of lipase inhibitors, making the active site accessible to solvent in the 3-D structures of several lipases including *Rhizomucor miehei* lipase (2, 3), *Thermomyces lanuginosus* lipase (4, 5), *Candida rugosa* lipase (6), human pancreatic lipase (HPL)<sup>1</sup> (7–9), and gastric lipase (10, 11). The structural differences observed between the closed and open lipase forms range from a relatively simple rigid hinge-type motion of a single helix in *R. miehei* lipase (3) to a much more complex pattern of multiple loops undergoing profound changes in their secondary structures (6, 9, 11). The proper active site arrangement, including the proper formation of the oxyanion hole, is affected by these conformations.

<sup>†</sup> The Structural Genomics Consortium is a registered charity (No. 1097737) that receives funds from the Canadian Institutes for Health Research, the Canadian Foundation for Innovation, Genome Canada through the Ontario Genomics Institute, GlaxoSmithKline, Karolinska Institutet, the Knut and Alice Wallenberg Foundation, the Ontario Innovation Trust, the Ontario Ministry for Research and Innovation, Merck & Co., Inc., the Novartis Research Foundation, the Swedish Agency for Innovation Systems, the Swedish Foundation for Strategic Research and the Wellcome Trust.

<sup>‡</sup> The coordinates of the two atomic structures of HPLRP2 reported in this paper have been deposited at the Protein Data Bank and are available using 2OXE and 2PVS PDB IDs.

\* Corresponding authors: CNRS UPR9025 Laboratoire d'Enzymologie Interfaciale et de Physiologie de la Lipolyse, Institut de Biologie Structurale et Microbiologie, 31, Chemin Joseph-Aiguier, 13402 Marseille Cedex 20, France. Tel: +33 4 91 16 41 34. Fax: +33 4 91 71 58 57. E-mail: carriere@ibsm.cnrs-mrs.fr, christian.cambillau@afmb.univ-mrs.fr.

<sup>§</sup> CNRS UPR9025 Laboratoire d'Enzymologie Interfaciale et de Physiologie de la Lipolyse.

<sup>||</sup> Laboratoire d'Architecture et Fonction des Macromolécules Biologiques, CNRS UMR6098.

<sup>⊥</sup> University of Toronto.

<sup>1</sup> Abbreviations: CVL, *Chromobacterium viscosum* lipase; DGDG, digalactosyldiglyceride; EPR, electron paramagnetic resonance; E600, diethyl p-nitrophenyl phosphate; HPL, human pancreatic lipase; MGDG, monogalactosyldiglyceride; MPD, 2-methyl-2,4-pentanediol; NaTDC, sodium taurodeoxycholate; PCL, *Pseudomonas cepacia* lipase; PL, pancreatic lipase; PLRP, pancreatic lipase-related protein; RDL, *Rhizopus delemar (oryzae)* lipase; TC3, tripropionin; YPD, yeast peptone dextrose culture medium.

mational changes. In HPL for instance, both the lid domain and the  $\beta$ 5 surface loop were shown to adopt a totally different conformation in the presence of phospholipids and bile salts (8). The  $\beta$ 5 loop folds back on the core of the protein, and this movement creates an electrophilic region close to the active site serine which stabilizes the negatively charged transition-state intermediate formed during ester hydrolysis. In lipases without a lid, like cutinase (12), the oxyanion hole is preformed. The lid structure in the classical lipases is therefore crucial both for substrate access to the active site and for adjusting the catalytic machinery.

The discovery of novel pancreatic lipase-related proteins (PLRP) has increased the complexity of structure–function relationships within this family of enzymes. Pancreatic lipase-related proteins 1 and 2 (PLRP1 and PLRP2) belong to the pancreatic lipase gene family, and they share 65–68% amino acid identity with the classical pancreatic lipase (PL) (13). Their structural components such as the catalytic triad (Ser-His-Asp) are highly conserved, and overall, the 3-D structures obtained so far are superimposable (14–16). A deletion within the lid domain was however observed in the PLRP2 from guinea pig (GPLRP2), which is able to accommodate more hydrophilic substrates than classical PL such as phospholipids and galactolipids with large polar heads (14). Besides this previously determined structural difference, PLRP also differs from classical PL by their biochemical and physiological properties. PLRP2 shows lipase, phospholipase A1 and galactolipase activities, whereas classical PL only shows lipase activity (17, 18) and PLRP1 is an inactive lipase against all known substrates (16). It was found that the galactolipase activity of the pancreatic juice is mainly due to PLRP2, the levels of which were found to be higher in herbivore species. These findings suggested a major role for PLRP2 in the digestion of the main lipids from plants (19–22). PLRP2 is also produced at a high level in species lacking pancreatic phospholipase A2, and it might also play a significant role in phospholipid digestion (17, 23). Unlike PL, which is only expressed in the exocrine pancreas, PLRP2 is expressed in various tissues in different species where it plays distinct physiological roles. Identification of rat PLRP2 (RPLRP2, also named GP-3) as a zymogen granule membrane-associated protein (24) suggested that RPLRP2 might be involved in the process of membrane fusion and the exocytosis of the secretory granule contents (25). The presence of mouse PLRP2 mRNA in interleukin-4 stimulated lymphocytes (26) and that of the mouse PLRP2 in intestinal Paneth cells (27) suggested that PLRP2 may be involved in the immune response. It was later shown that splenocytes from immunized PLRP2-deficient mice had a deficient killing activity and released lower levels of fatty acid from target cells than did control cells (28). Suckling PLRP2-deficient mice also showed fat malabsorption, and PLRP2 appeared to play a crucial role in the digestion of dietary fats in suckling animals (28). This effect is consistent with treatment with Orlistat/Xenical, an approved antiobesity drug which targets gastric and pancreatic lipases (29). Finally, PLRP2 was also identified in the seminal plasma of goat where it might also be involved in defense mechanisms by cleaning the genital tract (30, 31).

The differences observed in the kinetic properties of PLRP2 versus those of classical PL seem highly correlated with the structure of the lid domain, which has been shown

to be involved in substrate specificity by site-directed mutagenesis experiments (32). So far, crystal structures of pancreatic lipases with the lid in a functional open conformation were only observed in the presence of inhibitors, amphiphiles, or lipids. In this paper, we report the crystal structure of HPLRP2, the first structure of a pancreatic lipase with the lid in an open conformation obtained in the absence of amphiphiles. This new conformation of the lid was observed independently by two research groups in Toronto (Canada) and Marseille (France), which respectively solved the 3D structure of the wild-type HPLRP2 produced in insect cells and that of a nonglycosylated HPLRP2 mutant produced in yeast. These results are presented in this joint paper. The biochemical properties of HPLRP2 (inhibition by E600, absence of interfacial activation, activity on soluble substrate) suggest that the lid of HPLRP2 adopts this open conformation in solution.

## EXPERIMENTAL PROCEDURES

**Construction of the HPLRP2 Wild-Type Vector.** pAB-bee vector (AB Vector) was modified to allow for ligation-independent cloning using In-Fusion enzyme mediated directional recombination (Clontech). This vector was used to subclone a construct encoding the cDNA for HPLRP2 corresponding to the mature enzyme sequence in series with a noncleavable C-terminal (His)<sub>8</sub> tag. The vector also encodes for a honeybee melittin secretion signal sequence; after processing this sequence leaves one N-terminal alanine on the coding sequence. The mature enzyme is encoded by residues K18–C469. These residues are consequently numbered as K1–C452 in the text to reflect the residue numbering in the mature enzyme. The SF9 cell line (Invitrogen) was maintained using HyQ-SFX Insect Serum-Free medium (HyClone). The plasmid transfer vector was cotransfected into a 30–40% confluent monolayer of SF9 cells along with ProEasy linearized baculovirus DNA (AB Vector), using Cellfectin reagent (Invitrogen). Recombinant baculovirus was collected after 5 days of incubation at 27 °C. High titer viral stocks at stage of P3 were obtained by subsequently infecting SF9 cells at a density of 2 × 10<sup>6</sup> cells/mL in 6 well plates (Falcon) with P1 and P2 virus supernatants.

**Production of HPLRP2 in Insect Cells.** For large scale protein production from suspension cultures, High Five cells (Invitrogen) at a density of 2 × 10<sup>6</sup> cells/mL were infected with 1 mL of P3 viral stock for each 1 L of cell culture and incubated at 100 RPM and 27 °C. After 4 days of incubation cells were pelleted by centrifugation and culture medium containing the recombinant mature enzyme was collected. Media was brought to a pH of ~8 by adding 10X buffer A (50 mM Tris pH8, 500 mM NaCl, protease inhibitors (1 mM phenylmethanesulfonyl fluoride and Sigma general protease inhibitor P2714) and verifying pH of final solution. This was then mixed with 2–3 mL of HisLink Protein Purification Resin (Promega) per 250 mL of treated media. The mixture was incubated with mixing for at least 20 min at 4 °C. The treated media:resin mixture was spun at 500g for 3 min to pellet the HisLink resin. The supernatant was carefully decanted off the resin, and then 250 mL of buffer A was added to wash the resin. The resin was allowed to settle for 5 min, then poured off and washed 3 more times with fresh buffer A. The washed resin was then loaded onto a gravity

column and washed with 10 column volumes of buffer B (buffer A + 10 mM imidazole, pH 8). Samples were eluted from the HisLink resin by exposure to 10 mL elution buffer (buffer A + 500 mM imidazole and 10% glycerol). The eluate from the HisLink resin was diluted at least 10× by volume so that the final concentration of NaCl in the buffer was less than 50 mM. The protein was then loaded onto a 5 mL HiTrap Q HP column (GE Healthcare), washed with three column volumes of buffer C (50 mM Tris pH 8.0), and eluted over a linear gradient with buffer D (buffer C + 1 M NaCl). Peak fractions were pooled and concentrated using 15 mL Amicon concentrators with 10,000 MWCO (Millipore) to a final concentration of 10–15 mg/mL for crystallographic screening.

**Construction of the HPLRP2 N336Q Mutant Transfer Vector.** HPLRP2 cDNA, inserted into the pGAPZB *Pichia pastoris* transfer vector (pGAPZB-HPLRP2, 4289 bp (33)) was subjected to PCR using the QuikChange site directed mutagenesis kit (Stratagene), Pfu Ultra HF polymerase (Stratagene) and two different internal oligonucleotides with overlapping sequences (sense: GAACACAGGAGAGAG-TGGTCAATTACTAGTTGGAGATATAAGG; antisense: CCTTATATCTCCAACTAGTAAATTGACCACTCTCTC-CTGTGTT), specifically designed for introducing the N336Q mutation by transforming the N336 codon (AAC) into a Q codon (CAA). The PCR reaction included 18 cycles of denaturation at 95 °C for 30 s, hybridization at 54 °C for 1 min, and elongation at 68 °C for 5 min and was performed in a Mastercycler gradient thermocycler (Eppendorf). The cloning steps were performed in *Escherichia coli* XL1-blue strain, and cell cultures were grown in the presence of 25 µg/mL Zeocin. Plasmids DNA was isolated from *E. coli* cell cultures and purified using the NucleoBond Xtra Midipreps system (Machery-Nagel). DNA sequencing was carried out by Millegen (Paris, France).

**Transformation of the Yeast *Pichia pastoris*, Production and Purification of the HPLRP2 N336Q Mutant.** Electro-competent *Pichia pastoris* protease A deficient cells (SMD 1168 strain, Invitrogen) were prepared using standard methods (34) and transformed by electroporation using an electroporator 2510 (Eppendorf). Prior to the yeast transformation procedure, transformant plasmids were linearized with *Bsp*HI. The recombinant yeast clones were plated onto yeast peptone dextrose (YPD) 1% agar containing 100 µg/mL Zeocin and grown for 3–4 days at 30 °C. The most efficient N336Q HPLRP2 producing clone was then selected after screening the level of secretion of HPLRP2 N336Q in 5 mL of YPD medium containing 100 µg/mL Zeocin and incubated at 30 °C with orbital agitation at a rate of 100 rpm. Recombinant HPLRP2 secretion was estimated by measuring the lipase activity in the culture medium using tributyrin as a substrate in the presence of 0.1 mM NaTDC and colipase. The HPLRP2 N336Q mutant was then produced and purified as previously described for HPLRP2 (35).

**Lipase and Phospholipase Activity Measurements.** The lipase activities of HPLRP2 and rHPL were measured potentiometrically at 37 °C and pH 8.0 using the pH-stat technique (718 STAT Titrino, Metrohm), using vigorously stirred emulsions of acylglycerides (tributyrin, trioctanoin, triolein, diolein and monoolein) as substrate. The reaction vessel contained 0.5 mL of substrate dispersed in a 14.5 mL solution of 1 mM Tris-HCl buffer, pH 8.0 containing 0.1 M

NaCl, 5 mM CaCl<sub>2</sub>. When required, porcine pancreatic colipase purified from porcine pancreatic tissue (36) was added at a large molar excess.

Interfacial activation of HPLRP2 and HPL was investigated using tripalmitin (TC3; Acros organics) as the substrate and the pH-stat technique as previously described (37). The reaction vessel was thermostated at 37 °C and contained variable amounts of TC3, spanning concentration ranges in which TC3 is totally soluble (0–12 mM) or forms emulsion (>12 mM), in a 150 mM NaCl, 0.2% gum arabic (w/w) solution with a final volume of 15 mL.

The phospholipase activity of HPLRP2 was measured potentiometrically using purified egg L-α-phosphatidylcholine (Sigma) as substrate and the pH-stat technique (38). Specific activities were expressed as international lipase units (1 U = 1 µmol of fatty acid released per minute) per mg of enzyme.

The galactolipase activity was measured using monomolecular films of monogalactosyldiglyceride (MGDG; 1,2-di-O-dodecanoyl-3-O-β-D-galactopyranosyl-sn-glycerol) and digalactosyldiglyceride (DGDG; 3-O-(6-O-α-D-galactopyranosyl-β-D-galactopyranosyl)-1,2-di-O-dodecanoyl-sn-glycerol) as previously described (33, 35).

**Inhibition of HPLRP2 and rHPL by E600.** Inhibition experiments were performed with diethyl *p*-nitrophenyl phosphate (E600) in 50 mM sodium acetate buffer (pH 6.0) containing 50 mM NaCl and 5 mM CaCl<sub>2</sub>. HPLRP2 (52 µM) and HPL (20 µM) were incubated at 25 °C with E600 (Sigma, ref D 9286, stock solution at 4.16 M) at a lipase/inhibitor molar ratio of 1/85, in the presence and absence of 4 mM NaTDC and colipase at a molar ratio of 1/1. Residual lipase activity was measured at various incubation times using trioctanoin as substrate, in the presence of 0.1 mM NaTDC and a 2-fold molar excess of colipase in order to optimize the lipase activity measurements.

**Crystallization Conditions.** Crystals of wild-type HPLRP2 were obtained after screening against in-house crystallization screens in 96-well sitting drop format. Diffracting crystals were obtained from a hanging drop vaporization experiment at 18 °C by mixing protein at 15 mg/mL in equal volume ratio with the following precipitant solution: 1.17 M (NH<sub>4</sub>)<sub>2</sub>SO<sub>4</sub>, 0.1 M Na-cacodylate pH 5.5, 0.04 M NaCl. 15% glycerol was used as cryoprotectant.

Crystals of HPLRP2 N336Q mutant were obtained at room temperature using the vapor diffusion technique by mixing 6 µL of protein solution (14.5 mg/mL in 0.2 M NaCl, 25 mM Tris-HCl, pH 8.0) with 2 µL of 2.05 M ammonium sulfate, 0.1 M Hepes, pH 6.7. These crystals belong to the tetragonal space group I4<sub>1</sub>22 with unit cell dimensions  $a = b = 216.1 \text{ \AA}$ , and  $c = 123.6 \text{ \AA}$ . They contain two molecules per asymmetric unit, giving (assuming the molecular mass to be 50 kDa) a  $V_m = 3.5 \text{ \AA}^3/\text{Da}$  corresponding to a solvent content of 65% (39). Crystals were flash frozen to 100 K using Paratone-N as cryoprotectant.

**Data Collection and Processing.** Data from the wild-type HPLRP2 crystal were collected at 100 K on the IMCA-CAT beamline 17-ID at the Advanced Photon Source (Argonne National Laboratory) using an ADSC QUANTUM 210 detector ( $\lambda = 1.000 \text{ \AA}$ ). The data were indexed, integrated and scaled with HKL-2000 (40). Details of data collection and refinement are given in Table 1. Of note, the data exhibited a high degree of non-isomorphism in the resolution

Table 1: Data Collection, Structure Determination and Refinement Summary<sup>a</sup>

data set	HPLRP2	HPLRP2 N336Q
space group	I4 <sub>1</sub> 22	I4 <sub>1</sub> 22
unit cell	$a = b = 216.1 \text{ \AA}$ , $c = 123.6 \text{ \AA}$	$a = b = 216.1 \text{ \AA}$ , $c = 123.6 \text{ \AA}$
beamline	17-ID	ESRF ID14-3
wavelength	1.000	0.931
resolution	30.00–2.80	35.00–3.00
unique reflections	36137	28819
data redundancy	4.1 (4.1)	6.0 (5.8)
completeness <sup>b</sup>	99.3 (99.1)	99.2 (99.0)
$I/\sigma(I)$	12.7 (2.8)	11.2 (2.1)
$R_{\text{sym}}^c$	0.09 (0.78)	0.137 (0.78)
Refinement		
resolution	29.88–2.80	34.2–3.0
reflections used	34305	27791
all atoms {non-protein atoms}	6886 (72)	6977
$R_{\text{work}}/R_{\text{free}}^d$	0.22/0.26	0.193 (0.25)
rmse bond length	0.008	0.012
rmse bond angle	1.142	1.37
figure of merit	0.78	0.83
mean $B$ factor	68.8	51.5
MolProbity Ramachandran Analysis		
favored (%)	95.7	93.33
allowed (%)	99.9	99.20
outliers	1	7

<sup>a</sup> Atomic coordinates were deposited in the Protein Data Bank ([www.rcsb.org](http://www.rcsb.org)). PDB: 2OXE for wild-type HPLRP2 and 2PVS for HPLRP2 N336Q mutant. <sup>b</sup> Highest resolution shell is shown in parentheses. <sup>c</sup>  $R_{\text{sym}} = 100 \times \sum(|I - \langle I \rangle|)/\sum(\langle I \rangle)$ , where  $I$  is the observed intensity and  $\langle I \rangle$  is the average intensity from multiple observations of symmetry-related reflections. <sup>d</sup> The  $R_{\text{free}}$  value was calculated with 5% of the data.

range between 3 Å and 2.8 Å, leading to high  $R_{\text{sym}}$  in those shells (greater than 0.5). In these same resolution shells, the data was highly redundant and complete with  $I/\sigma$  of 3 or greater. Therefore, data extending to 2.8 Å was included in the scaling and refinement; most likely the non-isomorphism was due to high anisotropy in the crystal or other gross crystal defect.

Data on the HPLRP2 N336Q crystal were collected at 100 K from a single crystal in the beamline ID14-EH3 at the European Synchrotron Radiation Facility (ESRF Grenoble, France) using an ADSC Quantum 4 detector ( $\lambda = 0.931 \text{ \AA}$ ). The data were indexed and integrated using MOSFLM, scaled using SCALA and structure factor amplitudes were calculated using the TRUNCATE software program (41). The data processing statistics obtained at 3.0 Å resolution are given in Table 1.

**Phasing, Model Building and Refinement.** The structure of wild-type HPLRP2 was solved by the molecular replacement technique using data between 30 and 2.8 Å with the PHASER software program (42), part of the CCP4 Program Suite (41), using the structure of rat PLRP2 (PDB code 1BU8 (15)) as a starting model. Iterative manual rebuilding of the structure was carried out using the graphics program Coot (43) along with restrained refinement using the CCP4 program REFMAC (44). Solvent molecules were placed manually and by using the CCP4 program ARP/wARP (45). At later stages of the refinement TLS and restrained refinement was carried out using REFMAC (46), with the initial parameters obtained from the TLS Motion Determination server (47). The final model, with two molecules of the wild-type HPLRP2 in the asymmetric unit, has been refined to a working  $R$  factor of 0.22 and a free  $R$  factor of 0.26 for data between 29.88 and 2.80 Å (see Table 1).

The structure of HPLRP2 N336Q was solved by performing molecular replacement procedures taking data between a resolution of 35 and 3 Å with the AmoRe software program

(48), using the structure of rat PLRP2 (PDB code 1BU8 (15)) as a starting model. The electron density map obtained was readily interpretable, and the uncompleted model was finished based on the electron density map. Preliminary refinement was performed using REFMAC (44). Final refinement data are summarized in Table 1.

**Modeling of Digalactosyldiglyceride Molecule.** A DGDG molecule (3-O-(6-O- $\alpha$ -D-galactopyranosyl- $\beta$ -D-galactopyranosyl)-1,2-di-O-oleoyl-sn-glycerol) was built within the active site of HPLRP2 using the TURBO-FRODO software program (49). Most of the clashes observed could be eliminated by hand. A final docking was obtained with the REFMAC5 software program in the docking mode (50).

## RESULTS

**Production in Insect Cells and Purification of HPLRP2.** Recombinant wild-type HPLRP2 (HPLRP2) was secreted into the culture media by HighFive cells and purified to homogeneity using nickel-affinity chromatography followed by anion-exchange chromatography. LC-ESI-TOF mass spectrometry (Agilent) of HPLRP2 yielded a peak at 52815.3 ± 1 Da, corresponding to the theoretical mass of mature HPLRP2 (51857 Da, including the sequence derived from the vector) with one glycosylation event (958 Da).

**Production in Yeast and Purification of the HPLRP2 N336Q Mutant.** Recombinant HPLRP2 N336Q mutant and HPLRP2 were found to be secreted into the culture medium by the yeast *Pichia pastoris* with an apparent molecular mass of 50 kDa. The lipase was purified to homogeneity from the yeast culture media using the two-step purification procedure previously described for HPLRP2 (35). The protein elution profiles were similar to those previously obtained with HPLRP2 (data not shown). MALDI-TOF mass spectrometry analysis of the HPLRP2 N336Q mutant yielded a single peak corresponding to a mass of 50,352 ± 350 Da, which was

Table 2: Enzyme Activities of HPLRP2 N336Q Mutant, HPLRP2 and rHPL on Various Substrates<sup>a</sup>

substrate	HPLRP2				GPLRP2	rHPL		
	wild-type		N336Q			− colipase	+ colipase	
	− colipase	+ colipase	− colipase	+ colipase		0	0	
1(3)-monoolein	317 ± 11	317 ± 12	247 ± 26.4	290 ± 35	1239 ± 92	0	0	
1,2(2,3)-diolein	1.3 ± 0.6	5 ± 2	3.4 ± 0	3.6 ± 2	275 ± 13	0	2300 <sup>c</sup>	
triolein	5 ± 0	27.5 ± 13	4.3 ± 1.3	13 ± 2	41 ± 5	0	3200 <sup>c</sup>	
trioctanoin	43 ± 12	460 ± 16.3	40.2 ± 13	260 ± 9	0	0	6000 <sup>b</sup>	
tributyrin	287 ± 0	470.6 ± 16.3	212 ± 44	448 ± 62	1085 ± 63	0	8000 <sup>b</sup>	
egg PC	50.8 ± 3.7	nd	31.6 ± 5	nd	500 <sup>b</sup>	0	0	
MGDG	1.4 (18–25)	nd	nd	nd	3.5 (10–12)	0	0	
DGDG	3.2 (12)	nd	2.5 (12)	nd	2.5 (5–7)	0	0	

<sup>a</sup> Specific activities on glycerides and phospholipids were measured at pH 8.0, using the pH-stat technique. These activities are expressed in units (1 U = 1 μmol of fatty acid released per minute) per mg of enzyme. These experiments were carried out in triplicate in the presence of 4 mM NaTDC for glycerides or 20 mM DOC for phospholipids, and in the presence or absence of a 2-fold molar excess of colipase. Maximum activities on monogalactosyl diglycerides (MGDG) and digalactosyldiglycerides (DGDG) were measured using the monomolecular film technique. These activities are expressed in mole of substrate hydrolyzed min<sup>-1</sup> cm<sup>-2</sup> M<sup>-1</sup> where M is the molarity of the enzyme in the subphase of the monolayer trough. Values in brackets correspond to the surface pressures (mN m<sup>-1</sup>) at which these maximum activities were measured. nd: not determined. <sup>b</sup> Data adapted from Thirstup et al. (17). <sup>c</sup> Data from Eydoux et al. (35).

close to the theoretical mass of the mature HPLRP2 polypeptide (50,081 Da). This finding confirmed that the HPLRP2 N336Q mutant is not glycosylated and that only one N-glycosylation site (N336) out the two potential ones (N336, N411) is normally occupied by a glycan chain in HPLRP2 when this protein is produced in the yeast with a molecular mass of 52,343 ± 600 Da.

**Lipolytic Activities of HPLRP2 and HPLRP2 N336Q Mutant.** The catalytic properties of the HPLRP2 and HPLRP2 N336Q were investigated and compared with those of the classical human pancreatic lipase (rHPL) using several acylglycerides, L-α-phosphatidylcholine and galactolipids as substrates (Table 2). Using long and medium chain acylglycerides, HPLRP2 N336Q mutant and HPLRP2 displayed a much higher specific activity on monoolein than on diolein, triolein and trioctanoin, whereas rHPL had a reversed behavior on the same substrates, with no significant activity on monoolein. Using the partly soluble short chain tributyrin, the activity of both HPLRP2 N336Q mutant and HPLRP2 was found to be high in the presence of bile salts and in the absence of colipase, whereas rHPL was inactive under these conditions. Whatever the triglyceride substrate, HPL requires colipase to be active in the presence of micellar (>1–2 mM) bile salt concentration as shown in Figure 1A using tributyrin. Conversely, HPLRP2 does not require colipase to be active on tributyrin and addition of colipase has only a weak effect on this activity (Figure 1A). Since bile salts induce lipase desorption from the oil–water interface, these findings support the idea that HPLRP2 acts preferentially on tributyrin monomers or small aggregates (micelles) dispersed in solution compared to at oil–water interfaces. By contrast, rHPL is only active in the presence of colipase that anchors the lipase at the oil–water interface, which indicates that the presence of an insoluble emulsified substrate is required for HPL to be active.

Both HPLRP2 and HPLRP2 N336Q mutant showed a significant phospholipase A1 activity on mixed phospholipid–bile salt micelles, whereas HPL does not act on this substrate (Table 2). The phospholipase activity of HPLRP2 was however 1 order of magnitude lower than that measured with the guinea pig PLRP2 (GPLRP2).

Both HPLRP2 and HPLRP2 N336Q mutant hydrolyzed monomolecular films of monogalactosyl- and digalactosyl-

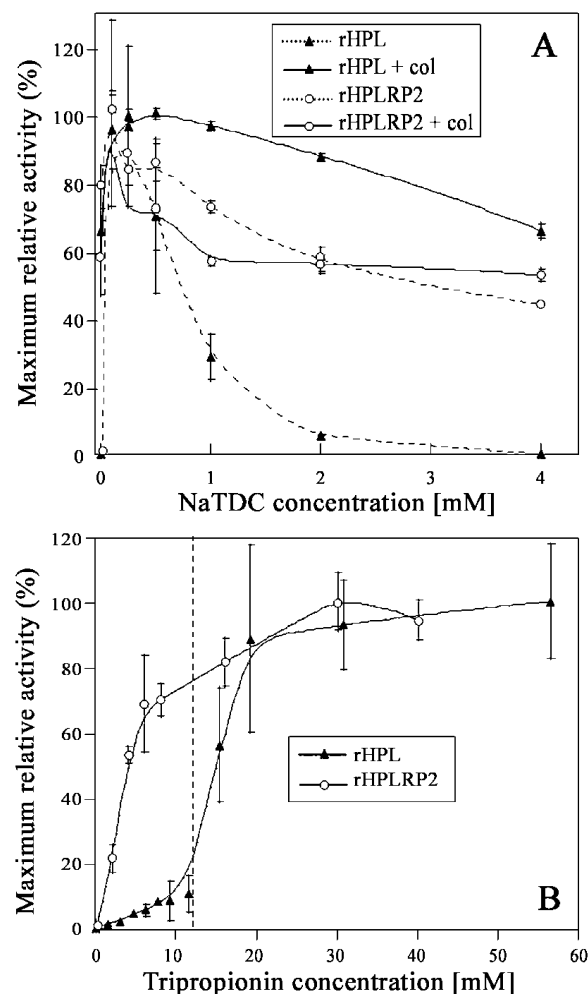


FIGURE 1: (A) Effects of NaTDC and colipase on the activity of HPLRP2 and rHPL. Lipolytic activities of HPLRP2 and rHPL were measured on emulsified tributyrin in the presence (full lines) and absence (broken lines) of colipase. (B) Effects of tripropionin concentration on the activities of HPLRP2 and rHPL. Lipase activities were measured using various tripropionin (TC3) concentrations (solution or emulsion) in the presence of a 2-fold excess of colipase. The vertical dashed line gives the solubility limit of tripropionin (12 mM).

diglyceride, whereas HPL did not (Table 2). Interestingly, the maximum galactolipase activities of HPLRP2 and GPLRP2 were of the same order of magnitude but HPLRP2

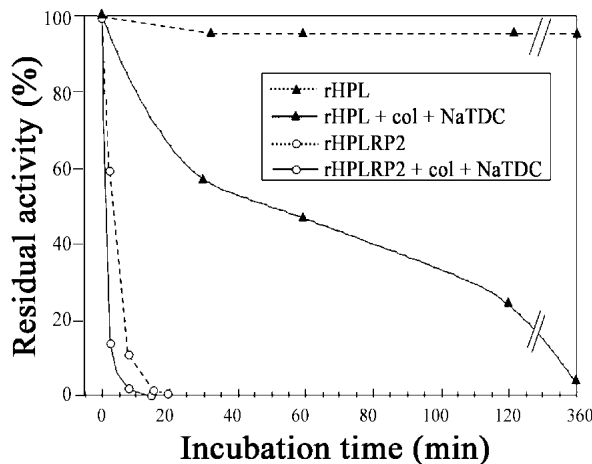


FIGURE 2: Inhibition of HPLRP2 and rHPL by E600. Residual activity of HPLRP2 and rHPL were determined using the pH-stat technique. The experiments on HPLRP2 and HPL were performed in the absence (broken lines) or presence (full lines) of 4 mM NaTDC and colipase at a colipase to lipase molar ratio of 1/1 in the incubation medium.

was found to display its maximum activity at higher surface pressures than GPLRP2, whatever the galactolipid substrate. These lipolytic activities measured with the monomolecular film technique (low values in Table 2) cannot be directly compared with the lipase and phospholipase activities measured with the pH-stat technique (high values in Table 2). One has to be aware however that the galactolipase activity of GPLRP2 on mixed galactolipid–bile salt micelles is of the same order of magnitude as the phospholipase activity (51) and that galactolipase activity is not a marginal activity of PLRP2 (33).

**Search for a Possible Interfacial Activation of HPLRP2.** To determine whether HPLRP2 presents the kinetic property of interfacial activation (52), its activity was assessed using the partly water-soluble tripalmitin (TC3) substrate at various concentrations and compared with that of rHPL (Figure 1B). At concentrations below the solubility limit of TC3 (12 mM), the activity of HPLRP2 reached around 70% of its maximum value, whereas HPL was only poorly active under the same conditions. The activity of HPLRP2 increased slowly above the solubility limit of TC3 and showed no activation. On the contrary, HPL displayed a low activity below the solubility of TC3 and a jump in the activity was observed once the TC3 solubility limit was exceeded (Figure 1B).

**Inhibition of HPLRP2 and rHPL by E600.** In the absence of bile salts and colipase, the time required to obtain 50% inactivation of HPLRP2 by E600 was 3 min, whereas rHPL was not significantly inhibited under the same conditions after a 7 h period of incubation (Figure 2). In the presence of 4 mM NaTDC and colipase, the rate of inhibition of HPLRP2 by E600 increased significantly and 50% inhibition was reached within 1 min. Under the same assay conditions, the rate of rHPL inhibition was higher than in the absence of NaTDC, but 1 h was however required to obtain 50% inhibition.

**Comparison of Wild-Type and Mutant Structures of HPLRP2.** The two crystal structures of HPLRP2 were determined independently. Wild-type HPLRP2 was solved to a resolution of 2.8 Å (PDB ID 2OXE) and was obtained

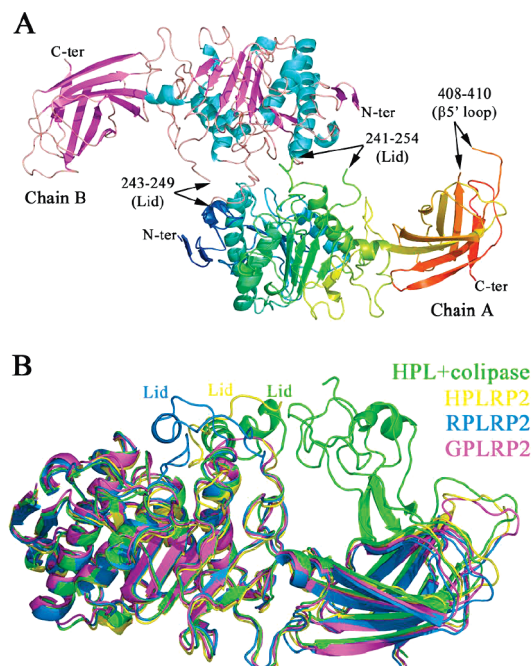


FIGURE 3: Structure of HPLRP2. A: View of the ribbon models of the two monomers of HPLRP2 observed in the crystal unit (PDB ID 2PVS).  $\alpha$  helices and  $\beta$  strands are shown in green and yellow in chain A and in blue and purple in chain B. Arrows indicate the limits of undefined amino acid residues. B: Ribbon view of the HPLRP2 structure superimposed on other known pancreatic lipase structures (HPL + colipase: classical human pancreatic lipase in its open conformation, with colipase interacting with the C-terminal domain and the lid. RPLRP2: rat pancreatic lipase-related protein 2. GPLRP2: 3D structure of the chimera made of the N-terminal catalytic domain of the guinea pig pancreatic lipase-related protein 2 and the C-terminal domain of HPL).

using a protein glycosylated at position N336 and secreted from insect cells. In contrast, the HPLRP2 N336Q structure was obtained at a resolution of 3.0 Å (PDB ID 2PVS). This mutant is not glycosylated and was expressed in the yeast *Pichia pastoris*. However, the overall structures and crystallographic statistics for both structures are strikingly similar. Both wild-type HPLRP2 and the N336Q mutant were solved in space group I4122 with identical cell dimensions ( $a = b = 216.9$  or  $216.1$  Å,  $c = 123.6$  Å). Both crystals contain two molecules in the asymmetric unit (65% solvent,  $V_m = 3.5$  Å<sup>3</sup>/Da).

For both models, ordered density begins at residue Lys1 and ends at Cys452 (the numbering used corresponds to the mature form of the enzyme). The wild-type HPLRP2 model has an average all-atom  $B$ -factor of 69 Å<sup>2</sup>. Regions of the model with  $B$  factors significantly higher than the average are roughly centered around residues T43–R73, K343–I358, Q373–A388, and F403–T423 in both chains. Residues K240–I250 in chain A and K240–D251 in chain B, and R408–S413 in chain A and R408–E414 in chain B, are disordered and not modeled in the wild-type HPLRP2 structure. Both monomers are highly superimposable with rmsd values of 0.48 Å over all atoms. For the mutant N336Q structure both molecules in the asymmetric unit show identical average  $B$ -factors (60 Å<sup>2</sup>); however, molecule B is more clearly defined than A (Figure 3A). Chain A is not visible between residues 241–254 (lid) and 408–410 (C-terminal domain  $\beta'$  loop) while chain B is interrupted only between residues 243 and 249 within the lid. The highly

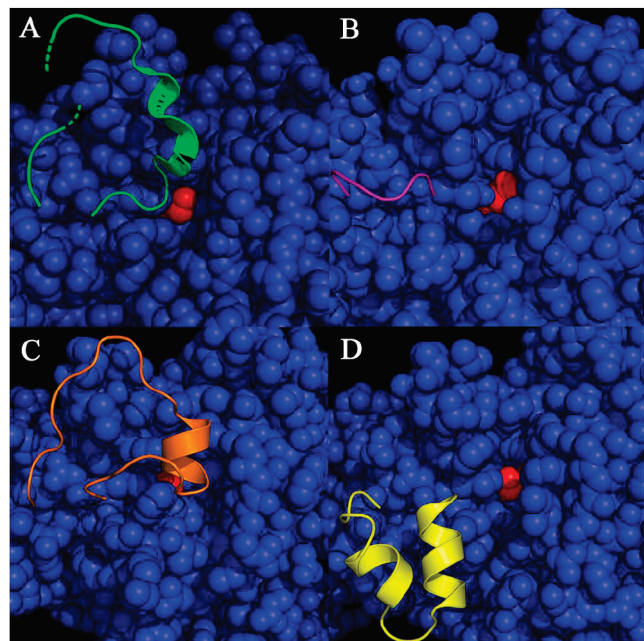


FIGURE 4: CPK views of pancreatic lipases with various lid conformations. A: HPLRP2 with the open lid shown in green. B: GPLRP2/HPL chimera, with its “mini-lid” shown in purple. C: HPL, with the lid in the closed conformation shown in orange. D: HPL, with the lid in the open conformation shown in yellow. The active site serine residue is shown in red. The lid domain secondary structure is represented as a ribbon model. The green dotted lines indicate the undefined section of the lid in the HPLRP2 structure.

hydrophobic  $\beta 5'$  loop region has previously been noticed to be poorly defined in the electron-density map of other pancreatic lipases (53). Again, both monomers are very similar and display rmsd values of 0.7 Å over all C $\alpha$  atoms. Differences in C $\alpha$  atom positions are mainly due to the occurrence of a small domain/domain rotation between the N- and C-termini, since the first 339 residues have an rmsd value of 0.24 Å. Both structures contain ordered density for ions; wild-type HPLRP2 is modeled with two calcium and five chloride ions in the asymmetric unit, and the mutant structure is modeled with two calcium and eight sulfate ions.

As with other pancreatic lipases, each monomer consists of two domains (Figure 3A). The N-terminal catalytic domain (residues 1 to 339) belongs to the  $\alpha/\beta$  hydrolase family fold, a large family of serine hydrolases with ubiquitous activities (54). The second domain, which belongs to the C2 family (55), is a  $\beta$ -sandwich running from residue 340 to 452. The active site, including the S154-H265-D178 catalytic triad, is freely accessible to solvent (Figure 4A), with the lid, located between C239 and C263, jutting out into the solvent and contacting the other monomer. The electron density map obtained for the lid was of poor quality and was interrupted in the case of both monomers. Since some proteolytic cleavage of HPLRP2 lid was previously observed upon storage (35), crystals were solubilized and analyzed using SDS-PAGE in the presence of DTT. The lid of the HPLRP2 N336Q mutant appeared to be partly cleaved (50% proteolysis), but no proteolysis was observed with the HPLRP2 produced in insect cells. The mass spectrometry analysis yielded masses of  $52,815.3 \pm 1$  Da for wild-type HPLRP2 (glycosylated) and  $50,352 \pm 350$  Da for HPLRP2 N336Q mutant (non-glycosylated), indicating that no additional

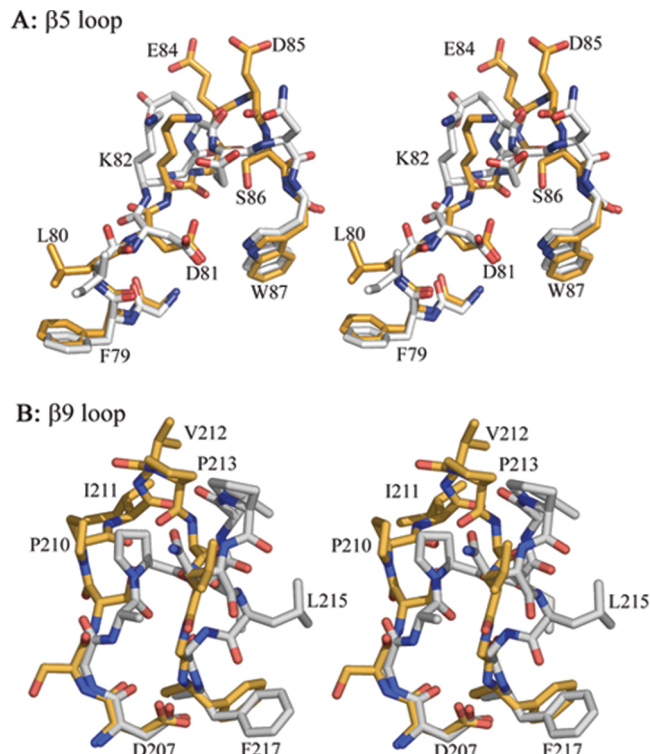


FIGURE 5: Stereoview of the  $\beta 5$  loop (A) and residues 207 to 217 of the  $\beta 9$  loop (B) of HPLRP2 (yellow) and HPL (white).

proteolytic cleavage had occurred. We also compared the kinetic properties of HPLRP2 N336Q mutant with those of the wild-type HPLRP2 (Table 2), and all these properties were found to be identical. It therefore seems that the poor quality of the density map in the lid domain is mainly due to dynamic disorder rather than proteolytic cleavage. In addition, the best definition of the lid is obtained in the chain B of HPLRP2 N336Q mutant with only 5 residues (244–248) missing. It is worth noticing that a limited proteolysis was found to occur in the horse PLRP2 lid domain between S245 and T246, and the structure of the lid could not be identified using X-ray diffraction data collected at 2.9 Å resolution (56).

The  $\beta 5$  loop (residues 78–86; Figure 5A) is found in the conformation forming the functional oxyanion hole, only observed so far in the 3-D structure of pancreatic lipases in which the lid was found in an open conformation (8, 9, 57) or was deleted (14). Whereas the residue F79 of HPLRP2, involved in the oxyanion hole together with L255, superimposes well with F77 of HPL, several residues of the  $\beta 5$  loop are found however at a different position when compared to the  $\beta 5$  loop of the open HPL (Figure 5A). The C $\alpha$  carbon atoms of D85 in HPLRP2 and E83 in HPL are distant from 4.7 Å, probably because the H-bond observed in HPL between E83 and W252 (lid) does exist in HPLRP2. Just downstream of the  $\beta 5$  loop, residue W87 of HPLRP2 superimposes well again with W85 of HPL. W87 is involved in a stacking with F269 of the HPLRP2 core, and this interaction is conserved in HPL (W85-Y267).

The overall structure of HPLRP2 superimposes well with those of other pancreatic lipases (Figure 3B), such as the HPL complexed with colipase in which the lid is in the open form (8); the GPLRP2/HPL chimera, in which the lid consists of a short loop of five amino acid residues instead of 23

amino acid residues in HPL (14); and rat PLRP2 lipase (RPLRP2), in which the lid is in the closed conformation (15). The rmsd values obtained between HPLRP2 and these three lipases range between 0.8 Å (HPL–colipase complex) and 1.1 Å (RPLRP2). These values are only slightly above the rmsd value calculated for HPLRP2 monomers. In both the GPLRP2/HPL chimera and the HPL–colipase complex, the active site is accessible to solvent (Figures 4B and 4D). In HPL, the lid uncovers the catalytic triad and the  $\beta$ 5 loop (residues 77–85 according to the HPL numbering) adopts a conformation which forms the oxyanion hole (F77 and L153). In RPLRP2, the lid was found to be in the “closed” conformation, which was previously observed in the case of classical pancreatic lipase alone (Figure 4C) (7, 53) and pancreatic lipase-related protein 1 (16), or in the absence of ligand in the HPL–colipase complex (58). One original and significant difference observed here between HPLRP2 and the other “open” lipases was the conformation of the  $\beta$ 9 loop (residues 205–225 according to the HPLRP2 numbering; Figure 5B), which is a crucial structural component involved in substrate binding (14). Two hydrophobic residues from the  $\beta$ 9 loop of HPL (L213, F215) were previously found to interact with the alkyl chain of a phosphonate inhibitor in the HPL–colipase complex, and these residues are probably involved in the stabilization of the acyl-enzyme intermediate formed during the lipolysis reaction (9). These residues are conserved (L215, F217) in the sequence of HPLRP2  $\beta$ 9 loop, but whereas F217 of HPLRP2 superimposes well with F215 of HPL, the C $\alpha$  carbon atoms of L215 in HPLRP2 and L213 in HPL are distant from 3.4 Å.

The excellent superimposition of the HPLRP2 structure with that of the open HPL–colipase complex made it possible to model with a good accuracy a molecule of C11 alkyl phosphonate inhibitor covalently bound to the active site S154 of HPLRP2, as it was experimentally observed in the HPL–colipase complex (9). The P=O group mimicking the C=O moiety of the reaction intermediate occupies a favorable position in the oxyanion hole, establishing hydrogen bonds with the N–H moiety of L155 and F79 (data not shown).

From the crystallographic data obtained with the wild-type HPLRP2 produced in insect cells, the glycosylation moiety at N336 was modeled as two *N*-acetyl-D-glucosamine and three  $\alpha$ -D-mannose groups. Interestingly, this short glycan chain characteristic of glycoproteins produced in insect cells (59) was found to lay down on the protein surface toward the C-terminal domain of HPLRP2 (Figure 6A). When the 3D structures of HPLRP2 and the HPL–colipase complex were superimposed, the glycan chain was found to clash with colipase at the level of its interaction with the C-terminal domain of HPL (Figure 6A). Glycosylation might therefore impair the interaction of HPLRP2 with colipase, like several amino acid mutations previously observed in the sequence alignment of the C-terminal domain of HPLRP2 with that of HPL (25). These findings support the weak effects of colipase on the lipase activity of HPLRP2 (Figure 1A; Table 2). No change in the effects of colipase was however observed when the lipase activity of the HPLRP2 N336Q mutant was measured (Table 2), suggesting that the presence of the glycan chain is not determinant for the weak effects of colipase and that this glycan chain probably adopts a different conformation in solution.

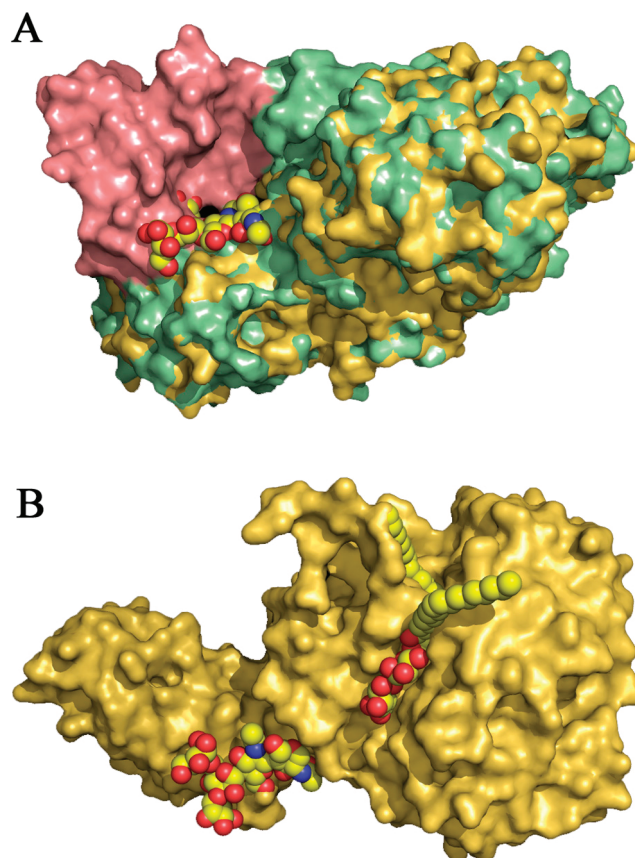


**FIGURE 6:** Glycosylation of HPLRP2 and docking of a galactolipid (DGDG) in the active site of HPLRP2. (A) Molecular surface representation of HPLRP2 (yellow) superimposed to the open HPL–colipase complex (HPL in green, colipase in pink). The glycan chain linked to N336 (GlucNac-GlucNac-Man-(Man)<sub>2</sub>) is shown as a CPK view. (B) Modeling of digalactosyl diglyceride in the active site of HPLRP2. Both the DGDG molecule and the glycan chain are shown as CPK views. The carbon atoms of the two oleoyl chains of the DGDG are shown in yellow.

Since HPLRP2 is one of the few galactolipases biochemically characterized to date, a digalactosyldiglyceride molecule was docked in the HPLRP2 structure (Figure 6B). HPLRP2 is able to accommodate a DGDG in its active site with the large digalactose polar head stabilized by interactions with aromatic residues (W87, F269). The cavity in which these residues are located is similar to that previously observed in the active site of the GPLRP2/HPL chimera (14), another enzyme with galactolipase activity (51). In both cases, the cavity results from differences in the lid in comparison with HPL. In HPL, this cavity is normally occupied by several residues involved in a network of interactions stabilizing the open conformation of the lid (D257–K268 salt bridge, R256–Y267 H-bond) and the  $\beta$ 5 loop (E83–W252 H-bond) (8). These interactions do not exist in HPLRP2 and the GPLRP2/HPL chimera. The DGDG molecule was modeled with the acyl chain at the *sn*-1 position laying on the  $\beta$ 9 loop, one of the acyl chain binding sites previously identified in HPL (8, 9). The second acyl chain was modeled in a cavity between the open lid and the  $\beta$ 5 loop, where it might be stabilized via apolar interactions with several aromatic amino acid residues (F96, Y272). An interesting finding is the location of the digalactosyl polar head of the DGDG on the same side of the HPLRP2 molecule as the glycan chain linked to N336.

## DISCUSSION

*Correlation between the Biochemical Properties of HPLRP2 and the Open Conformation of the Lid.* As a regulatory or security mechanism, the lid of classical pancreatic lipase controls access to the active site, adopting a closed conformation in the absence of substrates (amphiphiles), restricting solvent and other molecules from entering. However, the lid can open in solution in the presence of bile salts as demonstrated by various techniques including EPR spectroscopy of site-directed spin labels in the presence and absence of lipase inhibitors (60). These findings are consistent with the fact that crystal structures of classical pancreatic lipases with the lid in the open conformation have been obtained in the presence of mixed bile salt–phospholipid micelles (8) and nonionic detergents (57, 61). Pancreatic lipases therefore evolved a protective mechanism as a consequence of the lipophilic characteristics of its substrates. The finding that the lid of HPLRP2 was found to be in an open conformation in the crystal structure, without the requirement of detergents, lipids or substrate analogues, suggests that HPLRP2 adopts this conformation in solution. The biochemical properties of HPLRP2 support this hypothesis: (i) HPLRP2 clearly shows a preference for the soluble fraction of tributyrin and tripropionin (Figure 1), as well as for substrates forming small micellar aggregates in solution such as monolein and phospholipids (Table 2); (ii) HPLRP2 shows no interfacial activation, and its activity on tripropionin monomers is much higher than that of classical HPL (Figure 1); (iii) a fast rate of HPLRP2 inhibition by E600 is observed in the absence of bile salts (Figure 2), whereas E600 has no access to HPL active site under these conditions.

*General Comparison with Other PLRP2s.* The guinea pig PLRP2 was the first member of the PLRP2 subfamily to be biochemically characterized (17, 19, 51, 62–64). Like HPLRP2, GPLRP2 differed from classical pancreatic lipases in that it displayed no interfacial activation and was active on phospholipids and galactolipids. A large deletion was observed in the sequence corresponding to the lid, which was replaced by a short loop of 5 residues compared to 23 in the full-length lid of HPL (64). The 3-D structure of a chimeric lipase made of the N-terminal catalytic domain of GPLRP2 and the C-terminal domain of HPL revealed a solvent-accessible active site and a preformed oxyanion hole (14). From these observations and substrate modeling within the active site it was proposed that the phospholipase and galactolipase activities of GPLRP2 resulted from the deletion of the lid domain, thereby generating a larger and more polar active site in comparison with that of the triglyceride activity encoded by HPL. Exchange of HPL lid and GPLRP2 “mini-lid” by site-directed mutagenesis allowed for drastically reduced phospholipase activity for the GPLRP2 lid mutant, but phospholipase activity was not introduced in the HPL lid mutant (32). It was concluded that the lid domain was a necessary, but not the only, structural element contributing to the substrate specificity of pancreatic lipases (65).

GPLRP2 is the only PLRP2 identified so far with a deletion in the lid domain. All the other PLRP2s were also found to display both lipase and phospholipase activities with variable catalytic efficiency (17, 21, 31, 66). Since the coypu PLRP2 (CoPLRP2) did not display interfacial activation and

was highly active on the soluble fraction of tributyrin like GPLRP2, it was suggested that the full-length lid domain of CoPLRP2 might have an open conformation in solution (17). In contrast, the rat PLRP2 (RPLRP2) displayed interfacial activation and required bile salts to be inhibited by both diethyl *p*-nitrophenyl phosphate (E600) and tetrahydro-lipstatin, suggesting that the lid was closed in solution. The crystal structure of RPLRP2 confirmed that the lid domain was in a closed conformation in solution (15). These differences led to some confusion in the structure–function relationships of PLRP2s. The data obtained here with HPLRP2 indicates that the kinetic behavior of this enzyme is closer to that of CoPLRP2 than that of RPLRP2. These differences among PLRP2s might be explained by differences in the amino acid residues that are involved in the stabilization of the lid conformations in the classical HPL, most of these residues being mutated in PLRP2s. For instance, the open HPL lid interacts with the core of the protein through a salt bridge (D257–K268) and a hydrogen bond (R256–Y267). These four residues are substituted by G, G, F and E in HPLRP2, and interactions are no longer possible. Three of the four interacting residues are also mutated in CoPLRP2 whereas only two are mutated in RPLRP2.

*Specific Comparison between HPLRP2 and GPLRP2.* Although they differ in the size of their respective lids, HPLRP2 and GPLRP2 show similar kinetic properties, i.e. activities on acylglycerides, phospholipids and galactolipids, no interfacial activation (64) and direct inhibition by lipase inhibitors without the need for amphiphiles (67). The lipase and phospholipase activities of HPLRP2 were lower than those of GPLRP2, but their activities on MGDG and DGDG measured with the monomolecular film technique were of the same order of magnitude (Table 2). Docking of a DGDG molecule into the HPLRP2 structure showed that the presence of a full-length lid domain of 23 amino acid residues does not impair the access of the DGDG to the active site of HPLRP2, whereas the polar headgroup of DGDG cannot enter in the active site of HPL due to a different conformation of the lid. The cavity of HPLRP2 where the digalactosyl polar head fits has rather the same location as that observed in GPLRP2 (Figure 6). Since this cavity opens at the surface of the protein, it is envisioned that longer glycosyl groups might be docked within the active site of both HPLRP2 and GPLRP2. Moreover, several hydrophobic residues suspected to stabilize the substrate acyl chains in GPLRP2 and HPL are totally conserved in HPLRP2 (F79, Y116, L155, P181 and F217).

HPLRP2 and GPLRP2 differ however in the surface pressure at which they present their maximum activities on galactolipids: 18–25 mN/m on MGDG for HPLRP2 vs 10–12 mN/m for GPLRP2, and 12 mN/m on DGDG for HPLRP2 vs 5–7 mN/m for GPLRP2 (Table 2 and ref 35). The lid of HPLRP2 contains several hydrophobic residues that might increase the rate of enzyme adsorption at the lipid interface and its ability to act on monomolecular films at high surface pressures. The water accessible surface of the amino acid residues forming the lid was measured in HPLRP2, HPL and GPLRP2, and the hydrophilic/lipophilic balance (HLB) for the exposed residues of HPLRP2 lid (1.21) was found to be similar to that measured with HPL (0.8), whereas the mini-lid of GPLRP2 presented a higher HLB value (3.9). This finding may explain why GPLRP2 appears

to be less tensioactive than HPLRP2 in experiments with monomolecular films.

**Other Lipases with the Lid in an Open Conformation.** Other three-dimensional structures of lipases from bacteria have been determined in a totally or partially open conformation, suggesting that their lid could also be open in solution. Lang et al. (68) determined the crystal structure of a lipase from *Chromobacterium viscosum* (CVL; see PDB 1CVL) in which the lid was moving away from the catalytic groove and the oxyanion hole was formed, indicating that the lipase was in an active state. The active site residues were not exposed to the solvent, however, suggesting that CVL probably crystallized in an intermediate stage of the conformational transition from the inactive conformation with a closed lid to the active conformation with an open lid. This phenomenon was also observed in the structure of *Rhizopus delemar* (*oryzae*) lipase (RDL; see PDB 1TIC) (69). Two RDL molecules were present in the asymmetric unit; the first monomer shows the lid in a closed conformation whereas the second monomer exhibits the lid in an intermediary conformation as in CVL. The crystal structure of the *Pseudomonas cepacia* lipase (PCL) with the lid in an open conformation and the oxyanion hole formed was also obtained without the use of inhibitors by four independent groups (PDB 2LIP, 1OIL, 3LIP) (70, 71). Unlike HPLRP2, CVL and PCL were crystallized in the presence of 2-methyl-2, 4-pentanediol (MPD), which was suspected to stabilize the lipase in its open conformation. RDL was also crystallized in the presence of MPD, but in this case, no RDL monomers were found in an open conformation within the crystal (69). It is therefore not obvious that the opening of the lid domain can be attributed to MPD. It was also suggested that the crystal packing forces may have played a role in stabilizing the open conformation of the lid for these structures (70, 71). In the case of PCL and HPLRP2, the open lid is stabilized by both intra- and intermolecular contacts.

The structure of the lipase lid has always been a matter of discussion since the two first lipase structures were obtained in a closed conformation (2, 7), since this closed conformation could be an artifact due to protein crystal packing. Experiments carried out with inhibitors demonstrated that the lid could exist under different conformations both in crystals (3, 8) and in solution (60). Although there is no absolute evidence that the lid conformations observed in crystallization experiments reflect the lid structure in solution, the experimental data obtained here with HPLRP2 show good correlation since the kinetic properties indicate that the lid of HPLRP2 has to be opened in solution and that its open conformation has to be different from that observed in HPL in order to accommodate galactolipids in the active site. Overall, this study presents a new and significant step in the understanding of the lipase mechanism of action and substrate specificity.

## ACKNOWLEDGMENT

Use of the IMCA-CAT beamline 17-ID at the Advanced Photon Source was supported by the companies of the Industrial Macromolecular Crystallography Association through a contract with the Center for Advanced Radiation Sources at the University of Chicago. Use of the Advanced Photon

Source was supported by the U.S. Department of Energy, Office of Science, Office of Basic Energy Sciences, under Contract No. DE-AC02-06CH11357. Our thanks are also due to Mrs. Régine Lebrun and Danielle Moinier (Proteomic platform of the Institut de Biologie Structurale et Microbiologie, Marseille) for performing mass spectrometry and N-terminal sequence analysis of HPLRP2. The assistance of Jorge Rodriguez in performing the GPLRP2 activity assays is acknowledged.

## REFERENCES

- Aloulou, A., Rodriguez, J. A., Fernandez, S., Van Oosterhout, D., Puccinelli, D., and Carriere, F. (2006) Exploring the specific features of interfacial enzymology based on lipase studies. *Biochim. Biophys. Acta* **1761**, 995–1013.
- Brady, L., Brzozowski, A. M., Derewenda, Z. S., Dodson, E., Dodson, G., Tolley, S., Turkenburg, J. P., Christiansen, L., Huge-Jensen, B., Norskov, L., Thim, L., and Menge, U. (1990) A serine protease triad forms the catalytic centre of a triacylglycerol lipase. *Nature* **343**, 767–770.
- Brzozowski, A. M., Derewenda, U., Derewenda, Z. S., Dodson, G. G., Lawson, D. M., Turkenburg, J. P., Bjorkling, F., Huge-Jensen, B., Patkar, S. A., and Thim, L. (1991) A model for interfacial activation in lipases from the structure of a fungal lipase-inhibitor complex. *Nature* **351**, 491–494.
- Brzozowski, A. M., Savage, H., Verma, C. S., Turkenburg, J. P., Lawson, D. M., Svendsen, A., and Patkar, S. (2000) Structural origins of the interfacial activation in *Thermomyces* (*Humicola*) lanuginosa lipase. *Biochemistry* **39**, 15071–15082.
- Brzozowski, A. (1993) Crystallization of a *Humicola* lanuginosa lipase-inhibitor complex with the use of polyethylene glycol monomethyl ether. *Acta Crystallogr. D49*, 352–354.
- Grochulski, P., Bouthillier, F., Kazlauskas, R. J., Serreqi, A. N., Schrag, J. D., Ziomek, E., and Cygler, M. (1994) Analogs of reaction intermediates identify a unique substrate binding site in *Candida rugosa* lipase. *Biochemistry* **33**, 3494–3500.
- Winkler, F. K., d'Arcy, A., and Hunziker, W. (1990) Structure of human pancreatic lipase. *Nature* **343**, 771–774.
- van Tilburgh, H., Egloff, M.-P., Martinez, C., Rugani, N., Verger, R., and Cambillau, C. (1993) Interfacial activation of the lipase-procolipase complex by mixed micelles revealed by X-Ray crystallography. *Nature* **362**, 814–820.
- Egloff, M.-P., Marguet, F., Buono, G., Verger, R., Cambillau, C., and van Tilburgh, H. (1995) The 2.46 Å resolution structure of the pancreatic lipase-colipase complex inhibited by a C<sub>11</sub> alkyl phosphonate. *Biochemistry* **34**, 2751–2762.
- Roussel, A., Canaan, S., Egloff, M. P., Riviere, M., Dupuis, L., Verger, R., and Cambillau, C. (1999) Crystal structure of human gastric lipase and model of lysosomal acid lipase, two lipolytic enzymes of medical interest. *J. Biol. Chem.* **274**, 16995–17002.
- Roussel, A., Miled, N., Berti-Dupuis, L., Riviere, M., Spinelli, S., Berna, P., Gruber, V., Verger, R., and Cambillau, C. (2002) Crystal structure of the open form of dog gastric lipase in complex with a phosphonate inhibitor. *J. Biol. Chem.* **277**, 2266–2274.
- Martinez, C., Nicolas, A., van Tilburgh, H., Egloff, M.-P., Cudrey, C., Verger, R., and Cambillau, C. (1994) Cutinase, a lipolytic enzyme with a preformed oxyanion hole. *Biochemistry* **33**, 83–89.
- Giller, T., Buchwald, P., Blum-Kaelin, D., and Hunziker, W. (1992) Two novel human pancreatic lipase related proteins, hPLRP1 and hPLRP2. Differences in colipase dependence and in lipase activity. *J. Biol. Chem.* **267**, 16509–16516.
- Withers-Martinez, C., Carrière, F., Verger, R., Bourgeois, D., and Cambillau, C. (1996) A pancreatic lipase with a phospholipase A1 activity: crystal structure of a chimeric pancreatic lipase-related protein 2 from guinea pig. *Structure* **4**, 1363–1374.
- Roussel, A., Yang, Y., Ferrato, F., Verger, R., Cambillau, C., and Lowe, M. (1998) Structure and activity of rat pancreatic lipase-related protein 2. *J. Biol. Chem.* **273**, 32121–32128.
- Roussel, A., de Caro, J., Bezzine, S., Gastinel, L., de Caro, A., Carriere, F., Leydier, S., Verger, R., and Cambillau, C. (1998) Reactivation of the totally inactive pancreatic lipase RP1 by structure-predicted point mutations. *Proteins* **32**, 523–531.
- Thirstrup, K., Verger, R., and Carrière, F. (1994) Evidence for a pancreatic lipase subfamily with new kinetic properties. *Biochemistry* **33**, 2748–2756.

18. Carriere, F., Withers-Martinez, C., van Tilburgh, H., Roussel, A., Cambillau, C., and Verger, R. (1998) Structural basis for the substrate selectivity of pancreatic lipases and some related proteins. *Biochim. Biophys. Acta* 1376, 417–432.
19. Fauvel, J., Bonnefis, M. J., Sarda, L., Chap, H., Thouvenot, J. P., and Douste-Blazy, L. (1981) Purification of two lipases with high phospholipase A1 activity from guinea-pig pancreas. *Biochim. Biophys. Acta* 663, 446–456.
20. Thirstrup, K., Carrière, F., Hjorth, S. A., Rasmussen, P. B., Nielsen, P. F., Ladefoged, C., Thim, L., and Boel, E. (1995) Cloning and expression in insect cells of two pancreatic lipases and a procolipase from Myocastor coypus. *Eur. J. Biochem.* 227, 186–193.
21. Jayne, S., Kerfelec, B., Foglizzo, E., Chapus, C., and Cremon, I. (2002) High expression in adult horse of PLRP2 displaying a low phospholipase activity. *Biochim. Biophys. Acta* 1594, 255–265.
22. De Caro, J., Eydoux, C., Lebrun, R., Chérif, S., Gargouri, Y., Carrière, F., and De Caro, A. (2008) Occurrence of pancreatic lipase related protein 2 in various species and its relationship with herbivore diet. *Comp. Biochem. Physiol., Part B: Biochem. Mol. Biol.* 150, 1–9.
23. Fauvel, J., Bonnefis, M. J., Chap, H., Thouvenot, J. P., and Douste-Blazy, L. (1981) Evidence for the lack of classical secretory phospholipase A2 in guinea-pig pancreas. *Biochim. Biophys. Acta* 666, 72–79.
24. Wishart, M. J., Andrews, P. C., Nichols, R., Blevins, G. T., Jr., Logsdon, C. D., and Williams, J. A. (1993) Identification and cloning of GP-3 from rat pancreatic acinar zymogen granules as a glycosylated membrane-associated lipase. *J. Biol. Chem.* 268, 10303–10311.
25. Carrière, F., Thirstrup, K., Boel, E., Verger, R., and Thim, L. (1994) Structure-function relationships in naturally occurring mutants of pancreatic lipase. *Protein Eng.* 7, 563–569.
26. Grusby, M. J., Nabavi, N., Wong, H., Dick, R. F., Bluestone, J. A., Schotz, M. C., and Glimcher, L. H. (1990) Cloning of an interleukin-4 inducible gene from cytotoxic T lymphocytes and its identification as a lipase. *Cell* 60, 451–459.
27. Lowe, M. E. (2000) Properties and function of pancreatic lipase related protein 2. *Biochimie* 82, 997–1004.
28. Lowe, M. E., Kaplan, M. H., Jackson-Grusby, L., D'Agostino, D., and Grusby, M. J. (1998) Decreased neonatal dietary fat absorption and T cell cytotoxicity in pancreatic lipase-related protein 2 deficient mice. *J. Biol. Chem.* 273, 31215–31221.
29. Zambrowicz, B. P., and Sands, A. T. (2003) Knockouts model the 100 best-selling drugs—will they model the next 100? *Nat. Rev. Drug Discovery* 2, 38–51.
30. Pellicer-Rubio, M. T., Magallón, T., and Combarouñ, Y. (1997) Deterioration of goat sperm viability in milk extenders is due to a bulbourethral 60 kilodalton glycoprotein with triglyceride lipase activity. *Biol. Reprod.* 57, 1023–1031.
31. Sias, B., Ferrato, F., Pellicer-Rubio, M. T., Forgerit, Y., Guillouet, P., Leboeuf, B., and Carrière, F. (2005) Cloning and seasonal secretion of the pancreatic lipase-related protein 2 present in goat seminal plasma. *Biochim. Biophys. Acta* 1686 (3), 169–180.
32. Carrière, F., Thirstrup, K., Hjorth, S., Ferrato, F., Withers-Martinez, C., Cambillau, C., Boel, E., Thim, L., and Verger, R. (1997) Pancreatic lipase structure -function relationships by domain exchange. *Biochemistry* 36, 239–248.
33. Sias, B., Ferrato, F., Grandval, P., Lafont, D., Boullanger, P., De Caro, A., Leboeuf, B., Verger, R., and Carrière, F. (2004) Human pancreatic lipase-related protein 2 is a galactolipase. *Biochemistry* 43, 10138–10148.
34. Clegg, J. M., and Russell, K. A. (1998) Transformation. *Methods Mol. Biol.* 103, 27–39.
35. Eydoux, C., De Caro, J., Ferrato, F., Boullanger, P., Lafont, D., Laugier, R., Carrière, F., and De Caro, A. (2007) Further biochemical characterization of human pancreatic lipase-related protein 2 expressed in yeast cells. *J. Lipid. Res.* 48, 1539–1549.
36. Chapus, C., Desnuelle, P., and Foglizzo, E. (1981) Stabilization of the C-terminal part of pig and horse colipase by carboxypeptidase and trypsin inhibitors. *Eur. J. Biochem.* 115, 99–105.
37. Ferrato, F., Carrière, F., Sarda, L., and Verger, R. (1997) A critical reevaluation of the phenomenon of interfacial activation. *Methods Enzymol.* 286, 327–347.
38. Abousalham, A., and Verger, R. (2000) Egg yolk lipoproteins as substrates for lipases. *Biochim. Biophys. Acta* 1485, 56–62.
39. Matthews, B. W. (1968) Solvent content of protein crystals. *J. Mol. Biol.* 33, 491–497.
40. Otwinowski, Z., and Minor, W. (1997) Processing of X-ray Diffraction Data Collected in Oscillation Mode, in *Macromolecular Crystallography, Part A* (Carter Jr., C. W., and Sweet, R. M., Eds.) pp 307–326, Academic Press, New York.
41. The SERC collaborative computing project No. 4 from Daresbury Laboratory, U. (1994) The CCP4 Suite: Programs for Protein Crystallography. *Acta Crystallogr. D50*, 760–763.
42. McCoy, A. J., Grosse-Kunstleve, R. W., Adams, P. D., Winn, M. D., Storoni, L. C., and Read, R. J. (2007) Phaser crystallographic software. *J. Appl. Crystallogr.* 40, 658–674.
43. Emsley, P., and Cowtan, K. (2004) Coot: model-building tools for molecular graphics. *Acta Crystallogr. D60* 2126–2132.
44. Murshudov, G. N., V., and Dodson, E. J. (1997) Refinement of Macromolecular Structures by the Maximum-Likelihood Method. *Acta Crystallogr. D53*, 240–255.
45. Lamzin, V. S., and Wilson, K. S. (1993) Automated refinement of protein models. *Acta Crystallogr. D49*, 129–147.
46. Winn, M., Isupov, M., and Murshudov, G. N. (2001) Use of TLS parameters to model anisotropic displacements in macromolecular refinement. *Acta Crystallogr. D57*, 122–133.
47. Painter, J., and Merritt, E. A. (2006) TLSMD web server for the generation of multi-group TLS models. *J. Appl. Crystallogr.* 39, 109–111.
48. Navaza, J. (1994) AMoRe. *Acta Crystallogr. A50*, 157–163.
49. Roussel, A., and Cambillau, C. (1989) Turbo-Frodo, in *Silicon Graphics Geometry Partners Directory* (Graphics, S., Ed.) pp 77–78, Silicon Graphics, Mountain View.
50. Vagin, A. A., Steiner, R. A., Lebedev, A. A., Potterton, L., McNicholas, S., Long, F., and Murshudov, G. N. (2004) REFMAC5 dictionary: organization of prior chemical knowledge and guidelines for its use. *Acta Crystallogr., Sect. D: Biol. Crystallogr.* 60, 2184–2195.
51. Andersson, L., Carrière, F., Lowe, M., Nilsson, A., and Verger, R. (1996) Pancreatic lipase-related protein 2 but not classical pancreatic lipase hydrolyzes galactolipids. *Biochim. Biophys. Acta* 1302, 236–240.
52. Sarda, L., and Desnuelle, P. (1958) Action de la lipase pancréatique sur les esters en émulsion. *Biochim. Biophys. Acta* 30, 513–521.
53. Bourne, Y., Martinez, C., Kerfelec, B., Lombardo, D., Chapus, C., and Cambillau, C. (1994) Horse pancreatic lipase - the crystal structure refined at 2·3 angstrom resolution. *J. Mol. Biol.* 238, 709–732.
54. Ollis, D. L., Cheah, E., Cygler, M., Dijkstra, B., Frolow, F., Franken, S. M., Harel, M., Remington, S. J., Silman, I., Schrag, J., Sussman, J. L., Verschueren, K. H. G., and Goldman, A. (1992) The  $\alpha/\beta$  hydrolase fold. *Protein Eng.* 5, 197–211.
55. Chahinian, H., Sias, B., and Carrière, F. (2000) The C-terminal domain of pancreatic lipase: functional and structural analogies with c2 domains. *Curr. Protein Pept. Sci.* 1, 91–103.
56. Mancheno, J. M., Jayne, S., Kerfelec, B., Chapus, C., Cremon, I., and Hermoso, J. A. (2004) Crystallization of a proteolyzed form of the horse pancreatic lipase-related protein 2: structural basis for the specific detergent requirement. *Acta Crystallogr., Sect. D: Biol. Crystallogr.* 60, 2107–2109.
57. Hermoso, J., Pignol, D., Kerfelec, B., Cremon, I., Chapus, C., and Fontecilla-Camps, J. C. (1996) Lipase activation by nonionic detergents. The crystal structure of the porcine lipase-colipase-tetraethylene glycol monooctyl ether complex. *J. Biol. Chem.* 271, 18007–18016.
58. van Tilburgh, H., Sarda, L., Verger, R., and Cambillau, C. (1992) Structure of the pancreatic lipase-procolipase complex. *Nature* 359, 159–162.
59. Thirstrup, K., Carrière, F., Hjorth, S., Rasmussen, P. B., Wöldike, H., Nielsen, P. F., and Thim, L. (1993) One-step purification and characterization of human pancreatic lipase expressed in insect cells. *FEBS Lett.* 327, 79–84.
60. Belle, V., Fournel, A., Woudstra, M., Ranaldi, S., Prieri, F., Thome, V., Curraut, J., Verger, R., Guigliarelli, B., and Carrière, F. (2007) Probing the Opening of the Pancreatic Lipase Lid Using Site-Directed Spin Labeling and EPR Spectroscopy. *Biochemistry* 46, 2205–2214.
61. Hermoso, J., Pignol, D., Penel, S., Roth, M., Chapus, C., and Fontecilla-Camps, J. C. (1997) Neutron crystallographic evidence of lipase-colipase complex activation by a micelle. *EMBO J.* 16, 5531–5536.
62. Fauvel, J., Chap, H., Roques, V., and Douste-Blazy, L. (1984) Substrate specificity of two cationic lipases with high phospholipase A1 activity purified from guinea pig pancreas. II. Studies on glycerophospholipids. *Biochim. Biophys. Acta* 792, 72–78.

63. Fauvel, J., Chap, H., Roques, V., Sarda, L., and Douste-Blazy, L. (1984) Substrate specificity of two cationic lipases with high phospholipase A1 activity purified from guinea pig pancreas. I. Studies on neutral glycerides. *Biochim. Biophys. Acta* 792, 65–71.
64. Hjorth, A., Carrière, F., Cudrey, C., Wöldike, H., Boel, E., Lawson, D. M., Ferrato, F., Cambillau, C., Dodson, G. G., Thim, L., and Verger, R. (1993) A structural domain (the lid) found in pancreatic lipases is absent in the guinea pig (phospho)lipase. *Biochemistry* 32, 4702–4707.
65. Carrière, F., Withers-Martinez, C., van Tilburgh, H., Roussel, A., Cambillau, C., and Verger, R. (1998) Structural basis for the substrate selectivity of pancreatic lipases and some related proteins. *Biochim. Biophys. Acta* 1376, 417–432.
66. Jennens, M. L., and Lowe, M. E. (1995) Rat GP-3 is a pancreatic lipase with kinetic properties that differ from colipase-dependent pancreatic lipase. *J. Lipid Res.* 36, 2374–2382.
67. Cudrey, C., van Tilburgh, H., Gargouri, Y., and Verger, R. (1993) Inactivation of pancreatic lipases by amphiphilic reagents 5-(Dodecylthio)-2-nitrobenzoic acid and tetrahydrolipstatin. Dependence upon partitioning between micellar and oil phases. *Biochemistry* 32, 13800–13808.
68. Lang, D., Hofmann, B., Haalck, L., Hecht, H. J., Spener, F., Schmid, R. D., and Schomburg, D. (1996) Crystal structure of a bacterial lipase from *Chromobacterium viscosum* ATCC 6918 refined at 1.6 angstroms resolution. *J. Mol. Biol.* 259, 704–717.
69. Derewenda, U., Swenson, L., Wei, Y. Y., Green, R., Kobos, P. M., Joerger, R., Haas, M. J., and Derewenda, Z. S. (1994) Conformational lability of lipases observed in the absence of an Oil-Water interface. Crystallographic studies of enzymes from the fungi *Humicola lanuginosa* and *Rhizopus delemar*. *J. Lipid Res.* 35, 524–534.
70. Schrag, J. D., Li, Y., Cygler, M., Lang, D., Burgdorf, T., Hecht, H.-J., Schmid, R., Schomburg, D., Rydel, T. J., Oliver, J. D., Strickland, L. C., Dunaway, C. M., Larson, S. B., Day, J., and McPherson, A. (1997) The Open Conformation of a *Pseudomonas* Lipase. *Structure* 5, 187–202.
71. Kim, K. K., Song, H. K., Shin, D. H., Hwang, K. Y., and Suh, S. W. (1997) The crystal structure of a triacylglycerol lipase from *Pseudomonas cepacia* reveals a highly open conformation in the absence of a bound inhibitor. *Structure* 5, 173–185.
72. Abdullah, K., Cromlish, W. A., Payette, P., Laliberte, F., Huang, Z., Street, I., and Kennedy, B. P. (1995) Human cytosolic phospholipase A(2) expressed in insect cells is extensively phosphorylated on ser-505. *Biochim. Biophys. Acta* 1244, 157–164.

BI8005576